# Towards High-Precision Nuclear Forces from Chiral Effective Field Theory

**Evgeny Epelbaum**

*Ruhr-Universität Bochum, Fakultät für Physik und Astronomie, Institut für Theoretische Physik II, D-44780 Bochum, Germany*

**Abstract**

Chiral effective field theory is being developed into a precision tool for low-energy nuclear physics. I review the state of the art in the two-nucleon sector, discuss applications to few-nucleon systems and address challenges that will have to be addressed over the coming years.

**Keywords:** *Effective field theory, chiral perturbation theory, nuclear forces, few-nucleon systems*

## 1 Introduction

Chiral effective field theory (EFT) is widely applied to studies of low-energy structure and dynamics of nuclear systems. The method relies on the spontaneously broken approximate SU(2)×SU(2) chiral symmetry of QCD and allows one to compute the scattering amplitude of pions, the Nambu–Goldstone bosons of the spontaneously broken axial generators, with themselves and with matter fields via a perturbative expansion in momenta and quark masses, commonly referred to as the chiral expansion [1]. The appealing features of this method lie in its systematic and universal nature, which allows one to establish model-independent perturbative relations between low-energy observables in the Goldstone-boson and single-baryon sectors and low-energy constants (LECs) of the effective chiral Lagrangian.

When applied to self-bound systems such as atomic nuclei, the method outlined above has to be modified appropriately to account for the non-perturbative nature of the problem at hand by resumming certain parts of the scattering amplitude. According to Weinberg [2], the breakdown of perturbation theory is attributed to the appearance of time-ordered diagrams, which would be infrared divergent in the limit of infinitely heavy nucleons and are enhanced relative to their expected chiral order. The quantum mechanical Schrödinger equation provides a simple and natural framework to resum such enhanced contributions to the $A \geq 2$-nucleon scattering amplitude as it can be efficiently dealt with using a variety of available *ab initio* continuum methods [3–8], see the contributions of Petr Navrátil [9] and James Vary [10], or lattice simulations [11–13], see the contributions by Ulf-G. Meißner [14] and Dean Lee [15] for selected highlights and exciting new developments along this line. The problem

*Proceedings of the International Conference 'Nuclear Theory in the Supercomputing Era — 2018' (NTSE-2018), Daejeon, South Korea, October 29 – November 2, 2018, eds. A. M. Shirokov and A. I. Mazur. Pacific National University, Khabarovsk, Russia, 2019, p. 150.*

*http://www.ntse.khb.ru/files/uploads/2018/proceedings/Epelbaum.pdf.*

thus essentially reduces to the derivation of the nuclear forces and currents, defined in terms of the corresponding irreducible (i. e., non-iterative) parts of the amplitude, that are not affected by the above-mentioned enhancement and can be worked out order by order in the chiral expansion. The resulting framework, firmly rooted in the symmetries of QCD, allows one to derive consistent nuclear forces and currents and offers a systematically improvable theoretical approach to few- and many-nucleon systems [16–18].

Contrary to the on-shell scattering amplitudes, the nuclear forces and currents are scheme-dependent quantities, which are affected by unitary transformations or, equivalently, by nonlinear redefinitions of the nucleon field operators. Care is therefore required to maintain consistency between the two- and many-nucleon forces and the current operators, see Section 5 for the discussion. The unitary ambiguity in the resulting nuclear potentials is significantly reduced (but not completely eliminated) by the requirement of their renormalizability[1]. Another complication is related to the regularization of the Schrödinger or Lippmann–Schwinger (LS) equation [19]. Iterations of nuclear potentials in the LS equation generate ultraviolet divergent higher-order contributions to the amplitude, which cannot be made finite by counterterms in the truncated potential. One is, therefore, forced to keep the ultraviolet cutoff $\Lambda$ finite (of the order of the breakdown scale $\Lambda_b$) [19–21]. As discussed in Section 5, maintaining consistency between nuclear forces and currents in the presence of a finite cutoff is a rather nontrivial task starting from the fourth order in the chiral expansion.

In this contribution I will briefly review the current status of the chiral EFT, discuss a selected application and address the challenges that need to be tackled to develop this approach into a precision tool beyond the two-nucleon system.

## 2 Derivation of nuclear forces and currents

As already pointed out in the Introduction, the nuclear forces and currents are identified with the irreducible parts of the scattering amplitude and can be worked out using a variety of methods including matching to the $S$-matrix time-ordered perturbation theory (TOPT) and the method of unitary transformation (UT). The last approach has been pioneered in the fifties of the last century in the context of pion field theory [22, 23] and applied to the effective chiral Lagrangian in Refs. [24, 25]. The derivation of nuclear forces is achieved by performing a UT of the effective pion-nucleon Hamiltonian in the Fock space, which decouples the purely nucleonic subspace from the rest of the Fock space. The corresponding unitary operator is determined perturbatively by using the chiral expansion. The method can be formulated utilizing a diagrammatic language, but the resulting time-ordered-like graphs have a different meaning than the ones arising in the context of TOPT. The importance of any diagram can be estimated by counting the corresponding power $\nu$ of the chiral expansion parameter $Q \in \{p/\Lambda_b,\ M_\pi/\Lambda_b\}$, where $M_\pi$ denotes the pion mass and $p \sim M_\pi$ are three-momenta of the nucleons. For connected diagrams contributing to the $A$-nucleon potential with $B$ insertions of external classical sources, the chiral dimension $\nu$ is given

[1] Contrary to the on-shell $S$-matrix, loop contributions to the nuclear forces and currents may contain ultraviolet divergences which cannot be absorbed into the counterterms of the effective Lagrangian, see Section 5. When calculating the scattering amplitude, such divergences cancel against the ones generated by ladder diagrams, which emerge from iterations of the Lippmann–Schwinger equation.

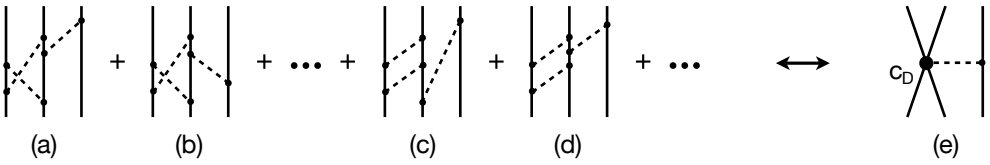


Figure 1: Time-ordered-like diagrams contributing to the two-pion-one-pion-exchange 3NF topology at the fourth order in the chiral expansion (graphs (a)-(d)) along with the one-pion-exchange-contact contribution to the 3NF at the third order. Solid and dashed lines refer to nucleons and pions, respectively. Solid dots and the filled circle denote vertices of dimension $\Delta = 0$ and $\Delta = 1$, respectively.

by [2, 26]

$$\nu = -4 - B + 2(A + L) + \sum_i V_i \Delta_i \,, \tag{1}$$

where $L$ is the number of loops and $V_i$ is the number of vertices of dimension $\Delta_i$ which appear in the diagram. The dimension of a vertex with $n_i$ nucleon field operators and $d_i$ derivatives/$M_\pi$-insertions/insertions of the external classical sources is defined according to [2] as

$$\Delta_i = d_i + \frac{1}{2} n_i - 2 \,. \tag{2}$$

The spontaneously broken chiral symmetry permits only interactions with $\Delta \geq 0$, so that a finite number of diagrams can be drawn at each finite chiral order $Q^\nu$. Notice that for actual calculations in the method of UT, it is more convenient to rewrite Eqs. (1), (2) using different variables as explained in Ref. [27].

As already pointed out above, loop contributions to nuclear potentials can, in general, not be renormalized. The problem is exemplified in Fig. 1 for the fourth-order (i. e., N$^3$LO) contribution to the three-nucleon force (3NF) proportional to $g_A^6$, with $g_A$ referring to the nucleon axial-vector constant. To obtain a renormalized expression for the 3NF, the loop integrals should involve only linearly divergent pieces, which can be cancelled by the counterterm in the LEC $c_D$. This is only possible if the pion exchange between the pair of the first two nucleons and the last nucleon in diagrams (a)-(d) factorizes out in order to match the expression for diagram (e) at the third chiral order (i. e., N$^2$LO). However, evaluating the corresponding diagrams in TOPT, one finds that the pion exchange does, actually, not factorize out. To ensure factorization of the one-pion exchange and enable renormalizability of the 3NF[2], a broad class of additional unitary transformations in the Fock space has been considered in Refs. [26, 27]. Other types of contributions to the 3NF at N$^3$LO and at the fifth order (N$^4$LO) in the chiral expansion and to the current operators show similar problems with renormalizability. So far, it was always possible to maintain renormalizability of nuclear forces and current operators, calculated using dimensional regularization (DR), via a suitable choice of additional unitary transformations, see Refs. [27–30] for more details.

Figure 2 visualizes the current state-of-the-art in the derivation of the nuclear Hamiltonian using the heavy-baryon formulation of chiral perturbation theory with

[2]The situation becomes more complicated if cutoff regularization is used instead of dimensional regularization, see the discussion in Section 5.

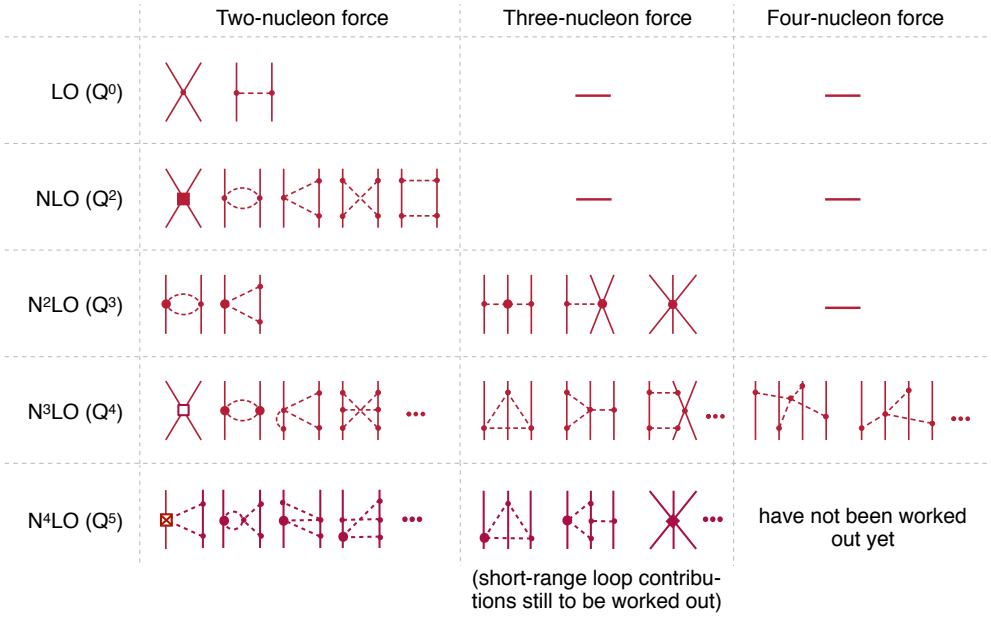


Figure 2: Chiral expansion of the nuclear forces. Solid and dashed lines refer to nucleons and pions. Solid dots, filled circles, filled squares, crossed squares and open squares denotes vertices from the effective chiral Lagrangian of dimension $\Delta = 0$, 1, 2, 3 and 4, respectively.

pions and nucleons as the only explicit degrees of freedom and utilizing the rules of naive dimensional analysis for few-nucleon contact operators, see Refs. [31–33] for alternative proposals. We remind the reader that all diagrams shown in this and following figures correspond to the irreducible parts of the scattering amplitude and to be understood as series of all possible time-ordered-like graphs for a given topology. As already explained before, the precise meaning of these diagrams and the resulting contributions to the nuclear forces are scheme dependent.

The nucleon-nucleon potential has been calculated to the fifth order ($\mathrm{N^4LO}$) in the chiral expansion using the dimensional regularization [24,34–41]. The expressions for the leading and subleading 3NF can be found in Refs. [42–46] and [26,27], respectively. Apart from the contributions involving $NN$ contact interactions, which still have to be worked out, the $\mathrm{N^4LO}$ terms in the 3NF can be found in Refs. [29, 47, 48]. The leading contribution to the four-nucleon force (4NF) appears at $\mathrm{N^3LO}$ and has been derived in Refs. [26,27]. It is important to emphasize that the long-range parts of the nuclear forces are completely determined by the spontaneously broken approximate chiral symmetry of QCD along with the experimental and/or empirical information on the pion-nucleon system needed to determined the relevant LECs in the effective Lagrangian. In this sense, the long-range contributions to the nuclear forces and currents can be regarded as parameter-free predictions. Given that the chiral expansion of the $NN$ contact operators in the isospin limit contains only contributions at orders $Q^{2n}$, $n = 0, 1, 2$, ..., the $\mathrm{N^2LO}$ and the isospin-invariant $\mathrm{N^4LO}$ corrections to the $NN$ potential are parameter-free. This also holds true for the $\mathrm{N^3LO}$ contributions to the 3NF and 4NF. For calculations utilizing a formulation of chiral EFT with explicit $\Delta(1232)$ degrees of freedom see Refs. [49–55].

The chiral power counting offers a natural qualitative explanation of the observed hierarchy of the nuclear forces, and the actual size of the various contributions to observables generally agrees well with the expectations based on naive dimensional analysis (NDA) underlying the chiral power counting. For example, the kinetic energy of the deuteron can naively be expected of the order of $E_{\rm kin} \sim M_\pi^2/m_N \sim 20$ MeV, since the pion mass is the only explicit soft scale in the problem. This compares well with the actual findings of $E_{\rm kin} \simeq 12 \,...\, 23$ MeV for the LO ... N$^4$LO chiral potentials of Ref. [56,57] and $E_{\rm kin} \simeq 12 \,...\, 16$ MeV for the LO ... N$^4$LO$^{+\,3}$ potentials of Ref. [58]. For comparison, for the Argonne AV18 potential [60], one finds $E_{\rm kin} \simeq 19$ MeV. For $^3$H, one can use the following simple considerations to estimate the size of the 3NF. Using phenomenological potentials, one typically finds $\big|\langle V_{NN}\rangle\big|_{^3{\rm H}} \sim 50$ MeV. Thus, according to the power counting, the 3NF contribution to the $^3$H binding energy may be expected of the order of $Q^3\big|\langle V_{NN}\rangle\big|_{^3{\rm H}}$. With $Q \sim M_\pi/\Lambda_b$ and $\Lambda_b \simeq 600$ MeV [56], one expects the 3NF to contribute about $0.013\big|\langle V_{NN}\rangle\big|_{^3{\rm H}} \sim 650$ keV to the triton binding energy. This matches well with the observed typical underbinding of $^3$H in calculations based on the $NN$ forces only [61,62]. Similar estimations may be carried out for the 4NF, for other light nuclei and for nucleon-deuteron scattering observables. In the latter case, assuming $Q = \max\{p/\Lambda_b,\ M_\pi/\Lambda_b\}$, one expects the 3NF effects to be small at low energy, but become more important at higher energies. Again, this expectation is in line with the observed discrepancies between nucleon-deuteron scattering data and calculations based on the $NN$ interactions only [61,62]. Notice, however, that the observed fine tuned nature of the nuclear force, resulting, e. g., in a small value of the deuteron binding energy of $E_{{\rm b},^2{\rm H}} \simeq 2.224$ MeV, cannot be explained by NDA which actually suggests $E_{{\rm b},^2{\rm H}} \sim E_{{\rm kin},^2{\rm H}} \sim \big|\langle V_{NN}\rangle\big|_{^2{\rm H}}$. On the other hand, one observes $\langle V_{NN}\rangle\big|_{^2{\rm H}} \simeq -E_{{\rm kin},^2{\rm H}}$, so that $E_{{\rm b},^2{\rm H}} \ll \big|\langle V_{NN}\rangle\big|_{^2{\rm H}}$. Similar fine tuning also persists for light nuclei.

Nuclear electromagnetic and axial currents have been worked out in chiral EFT completely up through N$^3$LO. Figure 3 summarizes the contributions to the electromagnetic charge and current operators derived using the method of UT in Refs. [28,63,64] and employing DR for loop integrals. The resulting expressions are, by construction, off-shell consistent with the nuclear forces derived by our group using the same approach. Again, the hierarchy of the $A$-nucleon contributions to the charge and current operators suggested by the chiral power counting is fully in line with empirical findings based on explicit calculations, which show the dominance of single-nucleon contributions for most of the low-energy observables [65,66]. In particular, the charge operator is strongly dominated by the one-nucleon (1N) term with the "meson-exchange" contributions being suppressed by four powers of the expansion parameter. On the other hand, the power counting suggests that the three-nucleon (3N) charge operator is as important as the two-body one, which can be tested, e. g., by calculating elastic form factors (FFs) of light nuclei. Notice further that up to N$^3$LO, the charge operator does not involve any unknown LEC. It is furthermore important to emphasize that the single-nucleon contributions to both the charge and current operators can be expressed in terms of the electromagnetic FFs of the nucleon. Using the available empirical information on the nucleon FFs then allows one to avoid relying on their strict chiral expansion known to converge slowly due to large contributions of vector mesons [67,68].

[3]The "+" sign indicates that we have included four contact interactions in $F$ waves from N$^5$LO in order to reproduce several sets of very precisely measured proton-proton data at higher energies. The same contact interactions are also included in the N$^4$LO potentials of Ref. [59].

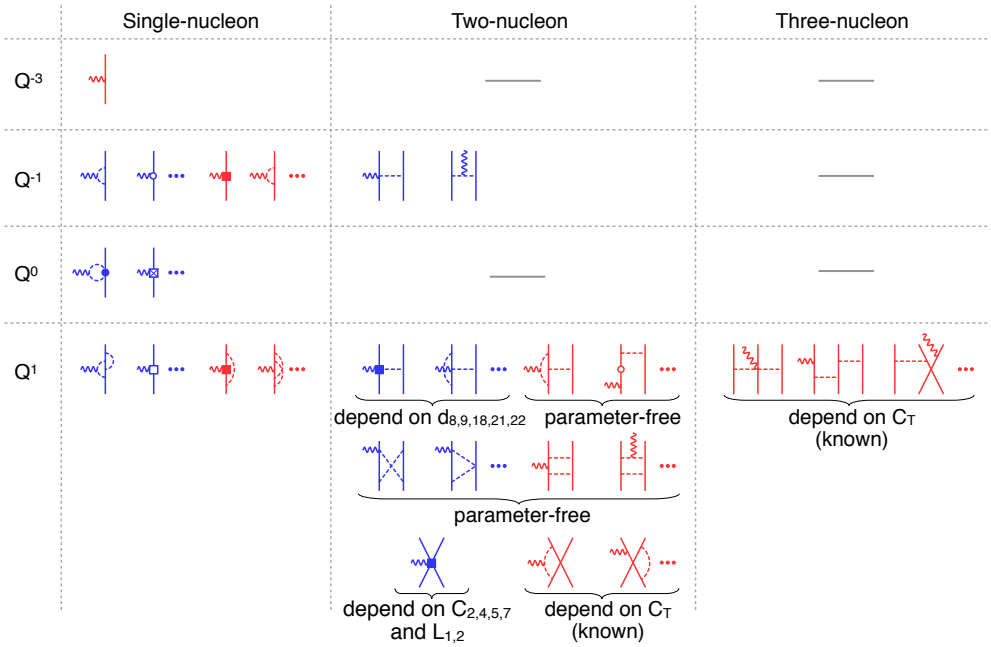


Figure 3: Chiral expansion of the nuclear electromagnetic currents. Red (blue) diagrams show the contributions to the charge (current) operators. Wavy lines refer to photons. For remaining notations see Fig. 2.

The leading contributions to the two-nucleon (2N) current operator emerge from a single pion exchange. The corrections at N$^3$LO include one-loop contributions to the one- and two-pion exchange as well as short-range operators. The third-order pion-nucleon LECs $d_{18}$ and $d_{22}$ can be determined from the Goldberger–Treiman discrepancy and the axial radius of the nucleon, while the $d_{9,21,22}$ contribute to the charged pion photoproduction and the radiative capture reactions [69, 70]. For the explicit form of the pion-nucleon Lagrangian see Ref. [71]. The short-range 2N operators depend, apart from the LECs $C_i$, which govern the short-range $NN$ potential at N$^2$LO, also on two new LECs $L_{1,2}$, which can be determined, e. g., from the deuteron magnetic moment and the cross section in the process $np \to d\gamma$ [72].

Notice that the expressions for the N$^3$LO contributions to the electromagnetic charge and current operators derived in the method of UT in Refs. [28, 63, 64] differ from the ones calculated by Pastore *et al.* using the TOPT [73–75]. The reader is referred to Ref. [76] for a comprehensive review article, which also addresses the differences between the two approaches.

Recently, these studies have been extended to derive the nuclear axial and pseudoscalar currents up to N$^3$LO using the method of UT [30], see Fig. 4. Interestingly, one observes exactly the opposite pattern as compared to the electromagnetic operators with the dominant contributions to the 1N current, 2N charge and 3N current operators appearing at LO, NLO and N$^3$LO, respectively. In a complete analogy with the electromagnetic currents, the 1N contributions are expressible in terms of the corresponding FFs of the nucleon. The 2N and 3N contributions to the current density are parameter-free at this order, while the long-range one-loop corrections to

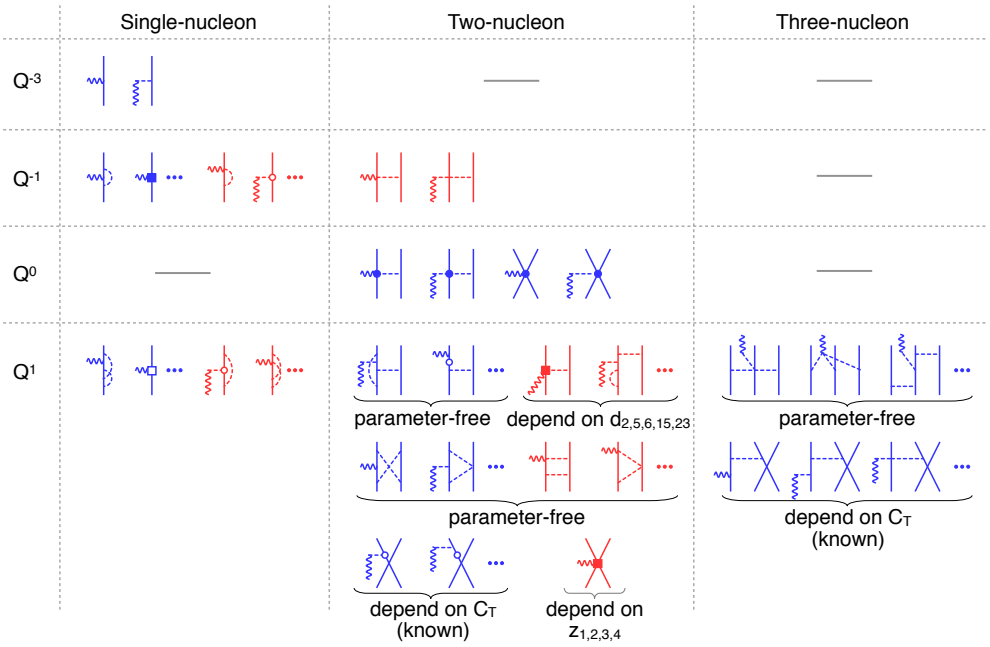


Figure 4: Chiral expansion of the nuclear axial currents. Red (blue) diagrams show the contributions to the charge (current) operators. Wavy lines refer to external axial-vector sources. For remaining notations see Fig. 2.

the 2N charge density depend on a number of poorly known LECs $d_i$. In addition, there are four new short-range operators contributing to the 2N charge operator at N$^3$LO. Again, we emphasize that our results deviate from the (incomplete) calculation by Baroni *et al.* [77] using TOPT and refer the reader to Ref. [76] for a detailed comparison.

## 3 High-precision chiral two-nucleon potentials

In the previous Section, I briefly reviewed the state of the art in the derivation of nuclear forces and currents. These calculations are carried out using DR to regularize divergent loop integrals. As pointed out in the Introduction, the derived nuclear potentials and current operators are singular at short distances and need to be regularized. To the best of my knowledge, it is not known how to subtract all ultraviolet divergences arising from iterations of the $NN$ potential in the Lippmann–Schwinger equation. Thus, the cutoff $\Lambda$ has to be kept finite of the order of the breakdown scale $\Lambda_b$ [19–21]. In Ref. [56], this scale was estimated to be $\Lambda_b \sim 600$ MeV. This was confirmed in the Bayesian analysis of Ref. [78], which found that it may even be somewhat larger, see Refs. [79,80] for a related recent work along this line. In practice, even lower values of the cutoff $\Lambda$ are preferred in order to avoid the appearance of deeply bound states, which would complicate the numerical treatment of the nuclear $A$-body problem, and to keep the potentials sufficiently soft in order to facilitate the convergence of many-body methods. It is, therefore,

important to use a regulator, which minimizes the amount of finite-cutoff artifacts. In Ref. [56], we argued that a local regularization of the pion-exchange contributions to the nuclear forces is advantageous compared to the nonlocal regulators used, e. g., in Refs. [25, 81, 82] as it maintains the analytic properties of the potential and does not induce long-range artifacts, see also Refs. [54, 83] for a related discussion. In Refs. [56, 57], a coordinate-space cutoff was employed to regularize the one- and two-pion exchange contributions. However, the implementation of such a regulator in coordinate space has turned out to be technically difficult for the 3NF and current operators. Thus, in Ref. [58], a momentum-space version of the local regulator was introduced by replacing the static propagators of pions exchanged between different nucleons via $(\vec{q}^{\,2}+M_\pi^2)^{-1} \longrightarrow (\vec{q}^{\,2}+M_\pi^2)^{-1}\exp\left[-(\vec{q}^{\,2}+M_\pi^2)/\Lambda^2\right]$, see Ref. [84] for a similar approach. Obviously, the employed regulator does not induce long-range artifacts at any finite order in the $1/\Lambda$-expansion. Notice further that the long-range part of the two-pion exchange $NN$ potential, derived using the DR, does not need to be recalculated using a new regulator. As shown in Ref. [58], the regularization of the two-pion exchange can be easily accounted for using the spectral-function representation. For example, for the central two-pion exchange potential $V(q)$, the regularization is achieved via

$$V(q) = \frac{2}{\pi}\int_{2M_\pi}^{\infty}\mu d\mu\,\frac{\rho(\mu)}{\vec{q}^{\,2}+\mu^2} + \ldots \longrightarrow \frac{2}{\pi}\int_{2M_\pi}^{\infty}\mu d\mu\,\frac{\rho(\mu)}{\vec{q}^{\,2}+\mu^2}\,e^{-\frac{\vec{q}^{\,2}+\mu^2}{2\Lambda^2}} + \ldots\,, \qquad (3)$$

where $\rho(\mu)$ is the corresponding spectral function and the ellipses refer to the contributions polynomial in $\vec{q}^{\,2}$ and $M_\pi$. In addition, a final number of (locally regularized) subtraction terms allowed by the power counting are taken into account to ensure that the corresponding long-range potentials and derivatives thereof vanish at the origin. For the contact $NN$ interactions, a simple non-local cutoff of the Gaussian type $\exp\left[-(\vec{p}^{\,2}+\vec{p}^{\,\prime 2})/\Lambda^2\right]$ with $\vec{p}$ and $\vec{p}^{\,\prime}$ denoting the initial and final center-of-mass momenta was employed. Using this regularization scheme and adopting the pion-nucleon LECs from the recent analysis in the framework of the Roy–Steiner equations [85,86], a family of new chiral $NN$ potentials from LO to N$^4$LO$^+$was presented in Ref. [58] for the cutoff values $\Lambda = \{350,\ 400,\ 450,\ 500,\ 550\}$ MeV. The resulting potentials at N$^4$LO$^+$ are currently the most precise chiral EFT $NN$ potentials on the market. For the medium cutoff choice of $\Lambda = 450$ MeV, the description of the neutron-proton and proton-proton scattering data from the 2013 Granada database [87] below $E_{\rm lab} = 300$ MeV is essentially perfect at N$^4$LO$^+$ as witnessed by the corresponding $\chi^2$ values of $\chi^2/\text{datum} = 1.06$ and 1.00, respectively. The N$^4$LO$^+$ potentials of Ref. [58] thus qualify to be regarded as partial wave analysis (PWA). Distinct features of these potentials in comparison with the other available chiral EFT interactions are summarized in Ref. [88].

As a representative example, we show in Fig. 5 the description of the neutron-proton scattering observables at $E_{\rm lab} \simeq 143$ MeV at various orders of the chiral expansion. The truncation bands have been generated using the algorithm formulated in Ref. [56]. For the application of the Bayesian approach for the quantification of truncation errors to the potentials of Ref. [58], see Ref. [88]. One observes excellent convergence of the chiral expansion and a very good agreement with the Nijmegen PWA. These conclusions also hold true for other scattering observables and deuteron properties.

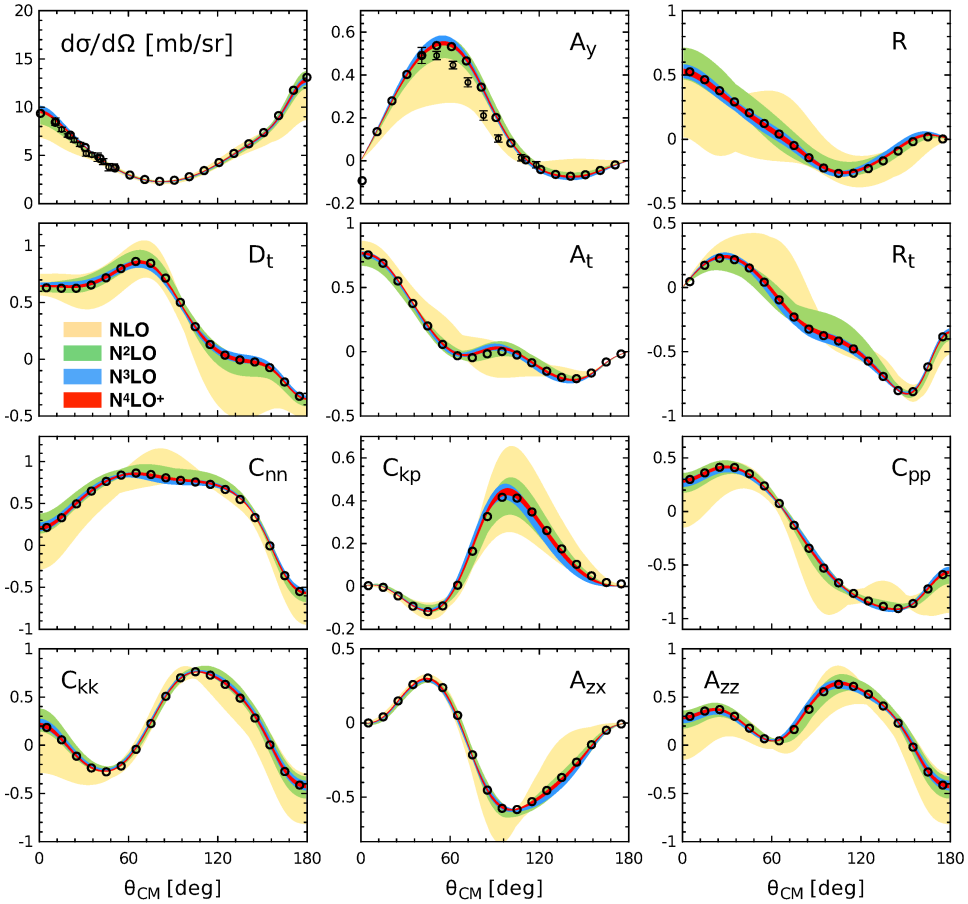


Figure 5: Neutron-proton scattering observables at $E_{\rm lab} = 143\,$MeV calculated up to N$^4$LO$^+$ using the chiral $NN$ potentials of Ref. [58] for the cutoff $\Lambda = 450\,$MeV. Data for the cross section are at $E_{\rm lab} = 142.8\,$MeV and are taken from Ref. [89] and those for the analyzing power $A_y$ are from Ref. [90]. Bands show the estimated truncation error while open circles are the results of the Nijmegen PWA [91].

# 4 Three-nucleon force

The novel semi-local chiral $NN$ potentials of Refs. [56–58] have already been explored in nucleon-deuteron scattering and selected nuclei [61, 62, 92–94]. By calculating various few-nucleon observables using the $NN$ interactions only, a clear discrepancies between experimental data and theoretical results well outside the range of the estimated uncertainties were observed. The magnitude of these discrepancies appears to be consistent with the expected size of the 3NF, which start contributing at N$^2$LO, see Fig. 2.

To perform complete calculations at N$^2$LO and beyond one needs to include the 3NF (and 4NF starting from N$^3$LO). These have to be regularized in a way *consistent* with the $NN$ potentials. The precise meaning of the *consistency* in this context will be addressed in the next section. In Ref. [95], we performed calculations of the

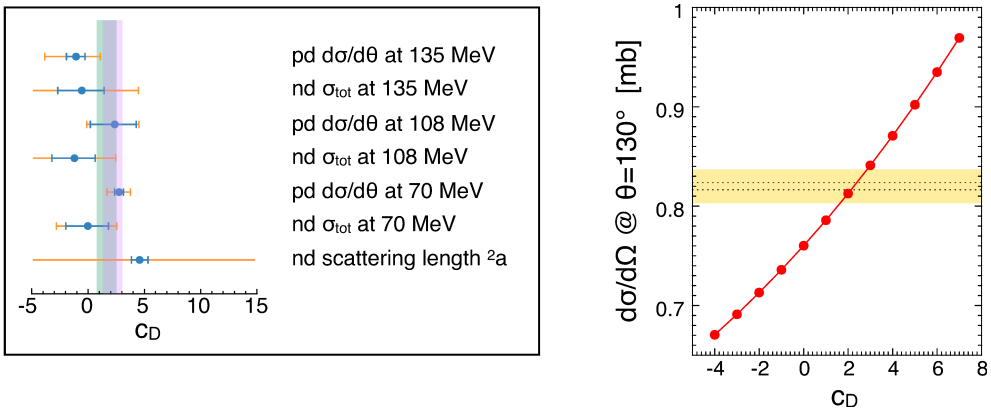


Figure 6: Left: Determination of the LEC $c_D$ from various $Nd$ scattering observables as explained in the text for the coordinate-space cutoff $R = 0.9$ fm. The smaller (blue) error bars correspond to the experimental uncertainty while the larger (orange) error bars also take into account the truncation error at N$^2$LO. Right: $Nd$ cross section in the minimum region ($\theta = 130°$) at $E_N = 70$ MeV as function of the LEC $c_D$. For each $c_D$ value, the LEC $c_E$ is adjusted to the $^3$H binding energy. Dotted lines show the statistical uncertainty of the experimental data from Ref. [99], while the yellow band also takes into account the quoted systematic uncertainty of 2%.

nucleon-deuteron ($Nd$) scattering and of the ground and low-lying excited states of light nuclei up to $A = 16$ up through N$^2$LO using the semilocal coordinate-space regularized $NN$ potentials of Refs. [56] together with the 3NF regularized in the same way. Notice that the Faddeev equations are usually solved in the partial wave basis. Partial wave decomposition of arbitrary 3NFs can be accomplished numerically using the machinery developed in Refs. [96,97]. The leading 3NF at N$^2$LO depends on two LECs, $c_D$ and $c_E$, which cannot be determined in the $NN$ system. It is customary to tune the short-range part of the 3NF in such a way that the $^3$H and/or $^3$He binding energies (BEs) are reproduced. As for the second constraint, different options have been explored including the neutron-deuteron spin-1/2 scattering length $^2a$, the BE and/or radius of the $\alpha$-particle, $Nd$ scattering observables, selected properties of light and medium-mass nuclei, equation of state for symmetric nuclear matter; see Ref. [98] for a review. In Ref. [95], we have explored the possibility to determine both LECs entirely from the three-nucleon system. Specifically, we used the triton BE to express $c_E$ as a function of $c_D$. To fix the $c_D$ value, a range of the available differential and total cross section data in elastic $Nd$ scattering and the doublet scattering length were considered. Notice that the 3NF is well known to have a large impact on the differential cross section in the minimum region (at not too low energies) [3]. Taking into account the estimated theoretical uncertainty from the truncation of the chiral expansion, very precise experimental data of Ref. [99] for the proton-deuteron differential cross section at $E_N = 70$ MeV were found to impose the strongest constraint on the $c_D$ value as visualized in Fig. 6. It is important to emphasize that contrary to the scattering length $^2a$ and the $^4$He BE, we do not observe any correlations between the triton BE and the cross section minimum in elastic $Nd$ scattering at the considered energies. In particular, we found that a variation of the $^3$H BE used in the fit

effects the value of $c_E$ but has almost no effect on the value of $c_D$. Having determined the LECs $c_D$ and $c_E$ as described above, the resulting nuclear Hamiltonian was used to calculate selected $Nd$ scattering observables and low-lying states in nuclei up to $A = 16$. The inclusion of the 3NF was found to improve the agreement with the data for most of the considered observables.

While these results are quite promising, the theoretical uncertainty of the N$^2$LO approximation is still fairly large [95]. At higher chiral orders, the estimated truncation errors are, however, expected to become significantly smaller than the observed deviations between the experimental data and theoretical calculations. This is especially true for the $Nd$ scattering observables at intermediate energies, see Ref. [61,62] for examples. Notice that the $Nd$ scattering observables are known to be not very sensitive to the off-shell behavior of $NN$ interactions as shown by Faddeev calculations using a variety of essentially phase-equivalent, high-precision phenomenological potentials [3]. This feature persists for the high-precision chiral $NN$ potentials at N$^4$LO$^+$. The large discrepancies between the theory and data for spin observables in $Nd$ scattering [100], therefore, seem to be universal and should presumably be attributed to the deficiencies of the available 3NF models. The 3NF effects at N$^2$LO appear to be qualitatively similar to the ones of the phenomenological models such as the Tucson–Melbourne [101] or Urbana IX [102] 3NFs and are insufficient to resolve the above mentioned discrepancies. The solution of the long-standing 3NF challenge is therefore likely to emerge from corrections to the 3NF beyond N$^2$LO. Based on the experience in the $NN$ sector [58], the description of $Nd$ scattering data will likely require pushing the chiral expansion to (at least) N$^4$LO.

# 5 Towards consistent regularization of nuclear forces and currents

To take into account the chiral 3NF in few-body calculations, the resulting expressions, derived using DR as discussed in Section 2, have to be regularized in the way *consistent* with the $NN$ force. As will be explained below, this poses a nontrivial problem starting from N$^3$LO, where the first loop contributions appear in the 3NF.

As already pointed out above, nuclear potentials and currents are not uniquely defined due to inherent unitary ambiguities. Off-shell behaviors of the 2NF and 3NF must be consistent in order to ensure that iterations of the Lippmann–Schwinger (or Faddeev) equations reproduce the corresponding on-shell contributions to the $S$-matrix (up to higher-order corrections), as exemplified in Fig. 7 for one particular contribution to the 3N scattering amplitude. As already mentioned before, all expressions for the nuclear forces and current operators reviewed in Section 2, which are derived using the method of UT and employing DR to regularize the divergent loop integrals, are consistent with each other *provided one also uses DR to regularize the loops from iterations of the integral equation*, see, e. g., the first diagram on the right-hand side of the equation in Fig. 7. However, in practice, regularization of the $A$-body Schrödinger equation in the context of nuclear chiral EFT is achieved by introducing a cutoff rather than by using DR. This raises an important question of whether the usage of nuclear potentials, derived in DR and subsequently regularized with a cutoff, still yields results which are consistent in the above-mentioned sense. It is easy to see that this is, generally, not the case by looking at the example shown in

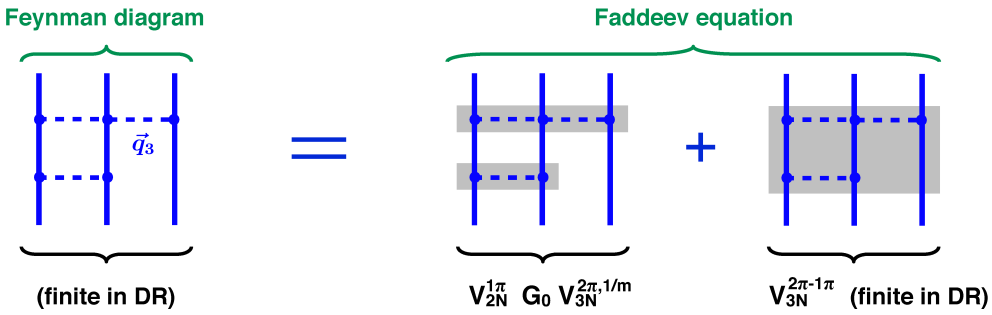


Figure 7: On-shell amplitude from the one-pion-two-pion-exchange Feynman diagram (left) is represented in terms of iterations of the Faddeev equation (right). Gray-shaded rectangles visualize the corresponding two- and three-nucleon potentials.

Fig. 7. The expressions for the two-pion-exchange 3NF proportional to $g_A^2/m_N$ in the second diagram are given in Eqs. (4.9)–(4.11) of Ref. [46], while the expression for the two-pion-one-pion exchange 3NF proportional to $g_A^4$ in the last diagram, evaluated in DR, can be found in Eqs. (2.16)–(2.20) of Ref. [45]. The one-pion exchange potential regularized with a local momentum-space cutoff discussed in Section 3 is given in Ref. [58]. Using the same regulator for the two-pion exchange 3NF, one finds that the $V_{2N}^{1\pi}\, G_0\, V_{3N}^{2\pi,\,1/m}$ contribution in Fig. 7 contains linear divergent terms of the kind

$$\sim \Lambda \frac{q_1^i q_3^j}{\vec{q}_3^{\,2} + M_\pi^2}, \qquad \sim \Lambda \frac{q_3^i q_3^j}{\vec{q}_3^{\,2} + M_\pi^2}\,. \tag{4}$$

While the last divergence can be absorbed into the LEC $c_D$, the first divergent term violates the chiral symmetry, since it corresponds to a derivative-less coupling of the exchanged pion. No such chiral-symmetry-breaking contribution appears in the 3NF at N$^2$LO. On the other hand, the Feynman diagram on the left-hand-side of the equation in Fig. 7 must, of course, be renormalizable not only in the DR but also using the cutoff regularization (provided it respects the chiral symmetry). The issue with the renormalization on the right-hand side of this equation is actually caused by using different regularization schemes when calculating the reducible (i. e., iterative) and irreducible contributions to the amplitude. Re-calculating $V_{3N}^{2\pi-1\pi}$ using the cutoff regularization instead of DR yields a linearly-divergent contribution, which cancels exactly the problematic divergence given by the first term in Eq. (4), and restores the renormalizability of the scattering amplitude (and the consistency). This example shows that a naive cutoff regularization of the 3NFs, derived using DR, is, in fact, inconsistent starting from N$^3$LO. Similar problems appear in calculations involving exchange currents, see Ref. [103] for the discussion and an explicit example.

It is important to emphasize that the above-mentioned problems do not affect calculations in the $NN$ sector (for the physical value of the quark masses). This is because the chiral symmetry does not impose constraints on the momentum dependence of the $NN$ contact interactions. It is, therefore, always possible to absorb all appearing ultraviolet divergences into a redefinition of the corresponding LECs. This is different for the contact interactions involving pion fields, which are indeed strongly constrained by the spontaneously broken chiral symmetry of QCD.

Last but not least, it is important to keep in mind that introducing a cutoff in a way compatible with the chiral and gauge symmetries is a rather nontrivial problem. The so-called higher-derivative regularization introduced by Slavnov in [104] provides one a possibility to implement a cutoff in the chirally invariant fashion already at the level of the effective Lagrangian, see Refs. [105–107] for applications in the context of chiral EFT.

# 6 Summary

There have been a remarkable progress in pushing the chiral EFT into a precision tool. This theoretically well-founded approach is firmly rooted in the symmetries of QCD and their breaking pattern. It allows one to address various low-energy hadronic reactions involving pions, nucleons and external sources in a systematically improvable fashion within a unified framework, thus putting nuclear physics onto a solid basis.

In this contribution, I focused mainly on the applications of chiral EFT in the few-nucleon sector. During the past two and a half decades, two-nucleon forces have been worked out completely up through $\mathrm{N^4LO}$ while the expressions for the 3NF, 4NF as well as the nuclear electromagnetic and axial currents are currently available at $\mathrm{N^3LO}$. The last generation chiral $NN$ potentials of Refs. [58, 59] benefit from the recent analysis of pion-nucleon scattering in the framework of the Roy–Steiner equation [85], which allows one to reconstruct the long-range part of the nuclear force in a parameter-free way. The resulting $\mathrm{N^4LO^+}$ potentials of Ref. [58] reach the same or even better quality in reproducing the $NN$ scattering data below the pion production threshold as the phenomenological high-precision potentials, but have $\sim$40% less adjustable parameters. This reduction signifies the importance of the two-pion exchange, which is completely determined by the spontaneous chiral symmetry of QCD along with the empirical information on the pion-nucleon system. Another important development concerns establishing a simple and reliable approach for estimating truncation errors [56, 57, 78–80], which usually dominate the error budget in chiral EFT, and exploring the other sources of uncertainties [58, 108, 109].

These developments in the $NN$ sector provide a solid basis for applications to heavier systems and/or processes involving electroweak probes. In contrast to the $NN$ force, the 3NFs are still poorly understood, and large discrepancies between the theory and data in the three-nucleon continuum pose a long-standing challenge in nuclear physics [100]. While the leading 3NF at $\mathrm{N^2LO}$ has already been extensively investigated in $Nd$ scattering and nuclear structure calculations and demonstrated to yield promising results, it is certainly insufficient to resolve the observed discrepancies. To include higher-order contributions to the 3NF (and the nuclear electroweak currents beyond $\mathrm{N^2LO}$), one needs to introduce a regulator in a way *consistent* with the 2NF, which poses a nontrivial problem starting from $\mathrm{N^3LO}$. Work along these lines is in progress. Another challenge that will have to be overcome is the determination of the LECs accompanying short-range contributions of the 3NF at $\mathrm{N^4LO}$, see Ref. [110] for an exploratory study.

## Acknowledgements

It is a great pleasure to thank all my collaborators, and especially Hermann Krebs and Ulf-G. Meißner, for sharing their insights into various topics discussed in this contribution and useful comments on the manuscript. I also thank the organizers of NTSE-2018 for making this interesting and stimulating workshop possible. This work was supported in part by DFG (SFB/TR 110, "Symmetries and the Emergence of Structure in QCD") and the BMBF (Grant No. 05P15PCFN1).

## References

[1] V. Bernard, N. Kaiser and U.-G. Meißner, Int. J. Mod. Phys. E **4**, 193 (1995).

[2] S. Weinberg, Phys. Lett. B **251**, 288 (1990).

[3] W. Glöckle *et al.*, Phys. Rep. **274**, 107 (1996).

[4] B. R. Barrett, P. Navratil and J. P. Vary, Prog. Part. Nucl. Phys. **69**, 131 (2013).

[5] G. Hagen *et al.*, Phys. Rev. Lett. **109**, 032502 (2012).

[6] H. Hergert *et al.*, Phys. Rev. C **87**, 034307 (2013).

[7] V. Soma, C. Barbieri and T. Duguet, Phys. Rev. C **87**, 011303 (2013).

[8] A. Lovato *et al.*, Phys. Rev. Lett. **111**, 092501 (2013).

[9] P. Navrátil, *Nuclear structure and dynamics from chiral forces*, talk given at the Int. Conf. 'Nuclear Theory in the Supercomputing Era — 2018' (NTSE-2018), October 29 – November 2, 2018, Daejeon, South Korea, http://ntse.khb.ru/files/uploads/2018/presentations/Navratil.pdf.

[10] P. Maris, I. J. Shin and J. P. Vary, *see these Proceedings*, p. 168, http://www.ntse.khb.ru/files/uploads/2018/proceedings/Vary.pdf.

[11] D. Lee, Prog. Part. Nucl. Phys. **63**, 117 (2009).

[12] D. Lee, Lect. Notes Phys. **936**, 237 (2017).

[13] T. A. Lähde, U.-G. Meißner, Lect. Notes Phys. **957**, 1 (2019).

[14] U.-G. Meißner, *see these Proceedings*, p. 28, http://www.ntse.khb.ru/files/uploads/2018/proceedings/Meissner.pdf.

[15] D. Lee, *see these Proceedings*, p. 45, http://www.ntse.khb.ru/files/uploads/2018/proceedings/Lee.pdf.

[16] E. Epelbaum, H. W. Hammer and U.-G. Meißner, Rev. Mod. Phys. **81**, 1773 (2009).

[17] E. Epelbaum and U.-G. Meißner, Annu. Rev. Nucl. Part. Sci. **62**, 159 (2012).

[18] R. Machleidt and D. R. Entem, Phys. Rep. **503**, 1 (2011).

[19] G. P. Lepage, nucl-th/9706029 (1997).

[20] E. Epelbaum and J. Gegelia, Eur. Phys. J. A **41**, 341 (2009).

[21] E. Epelbaum, A. M. Gasparyan, J. Gegelia and U.-G. Meißner, Eur. Phys. J. A **54**, 186 (2018).

[22] N. Fukuda, K. Sawada and M. Taketani, Prog. Theor. Phys. **12**, 156 (1954).

[23] S. Okubo, Prog. Theor. Phys. **12**, 603 (1954).

[24] E. Epelbaum, W. Glöckle and U.-G. Meißner, Nucl. Phys. A **637**, 107 (1998).

[25] E. Epelbaum, W. Glöckle and U.-G. Meißner, Nucl. Phys. A **671**, 295 (2000).

[26] E. Epelbaum, Phys. Lett. B **639**, 456 (2006).

[27] E. Epelbaum, Eur. Phys. J. A **34**, 197 (2007).

[28] S. Kölling, E. Epelbaum, H. Krebs and U.-G. Meißner, Phys. Rev. C **84**, 054008 (2011).

[29] H. Krebs, A. Gasparyan and E. Epelbaum, Phys. Rev. C **85**, 054006 (2012).

[30] H. Krebs, E. Epelbaum and U.-G. Meißner, Ann. Phys. (NY) **378**, 317 (2017).

[31] A. Nogga, R. G. E. Timmermans and U. van Kolck, Phys. Rev. C **72**, 054006 (2005).

[32] M. C. Birse, Phys. Rev. C **74**, 014003 (2006).

[33] M. P. Valderrama, Int. J. Mod. Phys. E **25**, 1641007 (2016).

[34] C. Ordonez and U. van Kolck, Phys. Lett. B **291**, 459 (1992).

[35] J. L. Friar and S. A. Coon, Phys. Rev. C **49**, 1272 (1994).

[36] N. Kaiser, R. Brockmann and W. Weise, Nucl. Phys. A **625**, 758 (1997).

[37] N. Kaiser, Phys. Rev. C **61**, 014003 (2000).

[38] N. Kaiser, Phys. Rev. C **62**, 024001 (2000).

[39] N. Kaiser, Phys. Rev. C **64**, 057001 (2001).

[40] N. Kaiser, Phys. Rev. C **65**, 017001 (2002).

[41] D. R. Entem, N. Kaiser, R. Machleidt and Y. Nosyk, Phys. Rev. C **91**, 014002 (2015).

[42] U. van Kolck, Phys. Rev. C **49**, 2932 (1994).

[43] E. Epelbaum *et al.*, Phys. Rev. C **66**, 064001 (2002).

[44] S. Ishikawa and M. R. Robilotta, Phys. Rev. C **76**, 014006 (2007).

[45] V. Bernard, E. Epelbaum, H. Krebs and U.-G. Meißner, Phys. Rev. C **77**, 064004 (2008).

[46] V. Bernard, E. Epelbaum, H. Krebs and U.-G. Meißner, Phys. Rev. C **84**, 054001 (2011).

[47] H. Krebs, A. Gasparyan and E. Epelbaum, Phys. Rev. C **87**, 054007 (2013).

[48] L. Girlanda, A. Kievsky and M. Viviani, Phys. Rev. C **84**, 014001 (2011).

[49] C. Ordonez, L. Ray and U. van Kolck, Phys. Rev. C **53**, 2086 (1996).

[50] N. Kaiser, S. Gerstendorfer and W. Weise, Nucl. Phys. A **637**, 395 (1998).

[51] H. Krebs, E. Epelbaum and U.-G. Meißner, Eur. Phys. J. A **32**, 127 (2007).

[52] E. Epelbaum, H. Krebs and U.-G. Meißner, Nucl. Phys. A **806**, 65 (2008).

[53] H. Krebs, A. M. Gasparyan and E. Epelbaum, Phys. Rev. C **98**, 014003 (2018).

[54] M. Piarulli *et al.*, Phys. Rev. C **91**, 024003 (2015).

[55] A. Ekström, G. Hagen, T. D. Morris, T. Papenbrock and P. D. Schwartz, Phys. Rev. C **97**, 024332 (2018).

[56] E. Epelbaum, H. Krebs and U.-G. Meißner, Eur. Phys. J. A **51**, 53 (2015).

[57] E. Epelbaum, H. Krebs and U.-G. Meißner, Phys. Rev. Lett. **115**, 122301 (2015).

[58] P. Reinert, H. Krebs and E. Epelbaum, Eur. Phys. J. A **54**, 86 (2018).

[59] D. R. Entem, R. Machleidt and Y. Nosyk, Phys. Rev. C **96**, 024004 (2017).

[60] R. B. Wiringa, V. G. J. Stoks and R. Schiavilla, Phys. Rev. C **51**, 38 (1995).

[61] S. Binder *et al.* (LENPIC Collaboration), Phys. Rev. C **93**, 044002 (2016).

[62] S. Binder *et al.* (LENPIC Collaboration), Phys. Rev. C **98**, 014002 (2018).

[63] S. Kölling, E. Epelbaum, H. Krebs and U.-G. Meißner, Phys. Rev. C **80**, 045502 (2009).

[64] H. Krebs, E. Epelbaum and U.-G. Meißner, Few-Body Syst. **60**, 31 (2019).

[65] H. Arenhovel and M. Sanzone, Few-Body Syst. Suppl. **3**, 1 (1991).

[66] J. Golak *et al.*, Phys. Rep. **415**, 89 (2005).

[67] B. Kubis and U.-G. Meißner, Nucl. Phys. A **679**, 698 (2001).

[68] M. R. Schindler, J. Gegelia and S. Scherer, Eur. Phys. J. A **26**, 1 (2005).

[69] H. W. Fearing, T. R. Hemmert, R. Lewis and C. Unkmeir, Phys. Rev. C **62**, 054006 (2000).

[70] A. Gasparyan and M. F. M. Lutz, Nucl. Phys. A **848**, 126 (2010).

[71] N. Fettes, U.-G. Meißner, M. Mojzis and S. Steininger, Ann. Phys. (NY) **283**, 273 (2000); Erratum: *ibid.* **288**, 249 (2001).

[72] J. W. Chen, G. Rupak and M. J. Savage, Nucl. Phys. A **653**, 386 (1999).

[73] S. Pastore, R. Schiavilla and J. L. Goity, Phys. Rev. C **78**, 064002 (2008).

[74] S. Pastore *et al.*, Phys. Rev. C **80**, 034004 (2009).

[75] S. Pastore, L. Girlanda, R. Schiavilla and M. Viviani, Phys. Rev. C **84**, 024001 (2011).

[76] H. Krebs, *Nuclear currents in chiral effective field theory, to be published in Eur. Phys. J. A.*

[77] A. Baroni *et al.*, Phys. Rev. C **93**, 015501 (2016); Erratum: *ibid.* **93**, 049902 (2016) and *ibid.* **95**, 059901 (2017).

[78] R. J. Furnstahl, N. Klco, D. R. Phillips and S. Wesolowski, Phys. Rev. C **92**, 024005 (2015).

[79] J. A. Melendez, S. Wesolowski and R. J. Furnstahl, Phys. Rev. C **96**, 024003 (2017).

[80] S. Wesolowski, R. J. Furnstahl, J. A. Melendez and D. R. Phillips, J. Phys. G **46**, 045102 (2019).

[81] E. Epelbaum, W. Glöckle and U.-G. Meißner, Nucl. Phys. A **747**, 362 (2005).

[82] D. R. Entem and R. Machleidt, Phys. Rev. C **68**, 041001 (2003).

[83] A. Gezerlis *et al.*, Phys. Rev. C **90**, 054323 (2014).

[84] T. A. Rijken, Ann. Phys. (NY) **208**, 253 (1991).

[85] M. Hoferichter, J. Ruiz de Elvira, B. Kubis and U.-G. Meißner, Phys. Rev. Lett. **115**, 192301 (2015).

[86] M. Hoferichter, J. Ruiz de Elvira, B. Kubis and U.-G. Meißner, Phys. Rep. **625**, 1 (2016).

[87] R. Navarro Perez, J. E. Amaro and E. Ruiz Arriola, Phys. Rev. C **88**, 064002 (2013); Erratum: *ibid.* **91**, 029901 (2015)].

[88] E. Epelbaum, *High-precision nuclear forces: Where do we stand?, to be published in Proc. Ninth Int. Workshop on Chiral Dynamics, 17–21 September 2018, Durham, NC, USA.*

[89] A. J. Bersbach *et al.*, Phys. Rev. D **13**, 535 (1976).

[90] A. F. Kuckes *et al.*, Phys. Rev. **121**, 1226 (1961).

[91] V. G. J. Stoks, R. A. M. Klomp, M. C. M. Rentmeester and J. J. de Swart, Phys. Rev. C **48**, 792 (1993).

[92] R. Skibiński *et al.*, Phys. Rev. C **93**, 064002 (2016).

[93] H. Witała *et al.*, Few-Body Syst. **57**, 1213 (2016).

[94] H. Witała *et al.*, Few-Body Syst. **60**, 19 (2019).

[95] E. Epelbaum *et al.* (LENPIC Collaboration), Phys. Rev. C **99**, 024313 (2019).

[96] J. Golak *et al.*, Eur. Phys. J. A **43**, 241 (2010).

[97] K. Hebeler, H. Krebs, E. Epelbaum, J. Golak and R. Skibiński, Phys. Rev. C **91**, 044001 (2015).

[98] H. W. Hammer, A. Nogga and A. Schwenk, Rev. Mod. Phys. **85**, 197 (2013).

[99] K. Sekiguchi *et al.*, Phys. Rev. C **65**, 034003 (2002).

[100] N. Kalantar-Nayestanaki, E. Epelbaum, J. G. Messchendorp and A. Nogga, Rep. Prog. Phys. **75**, 016301 (2012).

[101] S. A. Coon and H. K. Han, Few-Body Syst. **30**, 131 (2001).

[102] B. S. Pudliner *et al.*, Phys. Rev. C **56**, 1720 (1997).

[103] H. Krebs, *Electroweak current in chiral effective field theory, to be published in Proc. Ninth Int. Workshop on Chiral Dynamics, 17–21 September 2018, Durham, NC, USA.*

[104] A. A. Slavnov, Nucl. Phys. B **31**, 301 (1971).

[105] D. Djukanovic, M. R. Schindler, J. Gegelia and S. Scherer, Phys. Rev. D **72**, 045002 (2005)

[106] D. Djukanovic, J. Gegelia, S. Scherer and M. R. Schindler, Few-Body Syst. **41**, 141 (2007).

[107] J. Behrendt *et al.*, Eur. Phys. J. A **52**, 296 (2016).

[108] A. Ekström *et al.*, J. Phys. G **42**, 034003 (2015).

[109] R. Skibiński *et al.*, Phys. Rev. C **98**, 014001 (2018).

[110] L. Girlanda, A. Kievsky, M. Viviani and L. E. Marcucci, Phys. Rev. C **99**, 054003 (2019).